Cation and ligand roles in the coordination of Fe^{III} bisdithiolene complexes; the crystal structures of $(BrBzPy)_2[Fe(qdt)_2]_2$ and $[Fe(\alpha\text{-}tpdt)_2]_2^{2-}$ salts†

Ana Isabel Soares Neves, Isabel Cordeiro Santos, Dulce Belo and Manuel Almeida*

Received 4th August 2008, Accepted 8th January 2009
First published as an Advance Article on the web 7th February 2009
DOI: 10.1039/b813242a

The crystal structure of the new $(BrBzPy)_2[Fe(qdt)_2]_2$ complex (qdt = quinoxalinedithiolate) shows a rare weak Fe^{III} bisdithiolene dimerisation with unusual molecular planarity and long apical S–Fe distances. This anion configuration is intermediate between the only monomeric Fe bisdithiolene reported so far, with isolated square planar $[Fe(qdt)_2]^-$ units, and the common strong dimeric geometry also observed in other $[Fe(qdt)_2]_2$ salts. The standard strong dimeric situation is also observed in the $[Fe(\alpha\text{-}tpdt)_2]_2$ salt (α-tpdt = 2,3-thiophenedithiolate) with the same cation, as well as with *n*-Bu_4N and Et_4N showing the influence of different ligands and cations on the coordination geometry and supramolecular structure of the Fe^{III} complexes.

Introduction

At variance with the large diversity of coordination geometries and oxidation states of bisdithiolene complexes with most metals, the iron complexes with these ligands have essentially been restricted to one stable oxidation state, Fe(III),[1] and until quite recently all were found to adopt in the solid state the same square pyramidal, 4 + 1, coordination geometry due to the formation of dimeric arrangements through two Fe–S bonds between distorted square based $[Fe(S_2L)_2]^-$ units, $[Fe(S_2L)_2]_2^{2-}$. These units are characterised by having each an iron atom with 4 basal and one apical Fe–S bonds with distances in relatively narrow ranges of 2.21–2.25 Å and 2.44–2.49 Å, respectively. The first, and so far unique, exception to this rule was recently provided by us in the tetrabutylammonium salt of an iron bis-quinoxalinedithiolate complex, *n*-Bu_4N $[Fe(qdt)_2]$, displaying a perfectly square planar coordination geometry and a $S = 1/2$ spin state.[2] This effect was associated with specific cation interactions stabilizing the square planar configuration and hindering the usual dimerisation.

Aiming at a better understanding of the role of the cation *versus* the role of the ligand in the coordination geometry of Fe^{III} bisdithiolene complexes we have been exploring either new $[Fe^{III}(qdt)_2]^-$ salts with different cations or new iron complexes based on other bisdithiolene ligands (Scheme 1).

Following this strategy we report in this paper the crystal structure of the new salt $(BrBzPy)_2[Fe(qdt)_2]_2$, (BrBzPy = 1-(4′-bromobenzyl)pyridinium) which reveals an unusual coplanarity of the qdt ligands in the $Fe(qdt)_2$ monoanions and the formation of $[Fe(qdt)_2]_2$ dimeric dianions *via* relatively weak Fe–S apical bonds that are much longer (2.527(12) Å) than those observed in other dimers, suggesting an intermediate situation between previously known dimers and the monomer. The BrBzPy cation has a tendency to form stacks in the solid state and is known to favour the formation of segregated anion–cation structures.[3] The crystal structure of $(BrBzPy)_2[Fe(qdt)_2]_2$ is compared with that of a related new iron salt, with the same cation but based on the other ligand, α-tpdt = 2,3-thiophenedithiolate, that has previously been reported by us and combined with other metals:[4] $(BrBzPy)_2[Fe(\alpha\text{-}tpdt)_2]_2$. The crystal and molecular structure of this last compound is also compared with other salts of the new $[Fe(\alpha\text{-}tpdt)_2]$ dianion with other common cations such as tetrabutylammonium and tetraethylammonium in order to enlighten the roles of the ligand *versus* cation in the crystal engineering of these coordination complexes.

Results and discussion

$(BrBzPy)_2[Fe(qdt)_2]_2$ and $(BrBzPy)_2[Fe(\alpha\text{-}tpdt)_2]_2$

The X-ray structure analysis of $(BrBzPy)_2[Fe(qdt)_2]_2$ reveals that this compound crystallises in the triclinic space group *P*-1. Its crystal structure consists of centrosymmetric dianions $[Fe(qdt)_2]_2^{2-}$ and $(BrBzPy)^+$ cations forming pairs *via* inversion centres. The Fe^{III} atom presents the usual square pyramidal coordination (Fig. 1a), but in this case it is displaced towards the axial ligand only 0.310 Å from the S1, S2, S3 and S4 mean plane (Fig. 2a). This low displacement value is associated with an unusually large Fe–S apical distance of 2.527(12) Å when compared to the Fe–S apical distances in other dimerised Fe^{III} bisdithiolene complexes with other ligands or even with other qdt salts, usually in the range 2.4385–2.4884 Å (see Table 1).[2,5–10] The average basal Fe–S bond length in $(BrBzPy)_2[Fe(qdt)_2]_2$ is 2.2255(12) Å, within the usual range of values found in other square-pyramidal Fe^{III} dithiolate complexes.

The bond distances and angles in the qdt ligands were observed to be in the expected ranges as found in other complexes of this ligand. However in contrast with others Fe(III) dimers, where the ligands form quite a large dihedral angle, the

Dept. Química, Instituto Tecnológico e Nuclear/CFMCUL, P-2686-953 Sacavém, Portugal. E-mail: malmeida@itn.pt; Fax: +351219941455; Tel: +351219946171

† Electronic supplementary information (ESI) available: Tables of short contacts and hydrogen bonds in the crystal structure of $(BrBzPy)_2[Fe(qdt)_2]_2$, $(BrBzPy)_2[Fe(\alpha\text{-}tpdt)_2]_2$, $(n\text{-}Bu_4N)_2[Fe(\alpha\text{-}tpdt)_2]_2$ and $(Et_4N)_2[Fe(\alpha\text{-}tpdt)_2]_2$ (Tables S1, S2, S4 and S4). CCDC reference numbers 695832–695835. For ESI and crystallographic data in CIF or other electronic format see DOI : 10.1039/b813242a

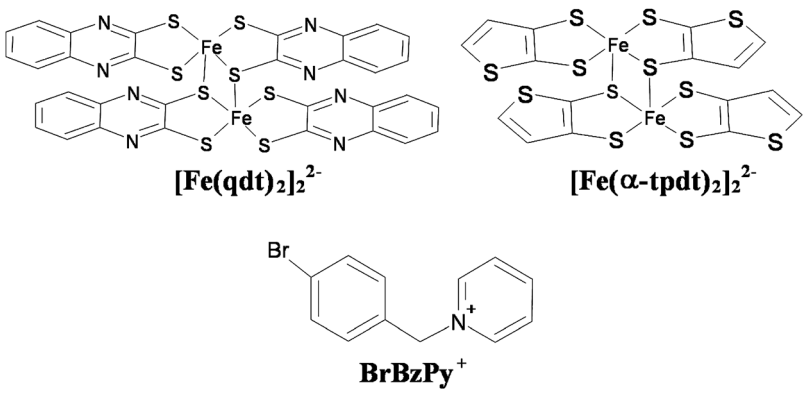

Scheme 1

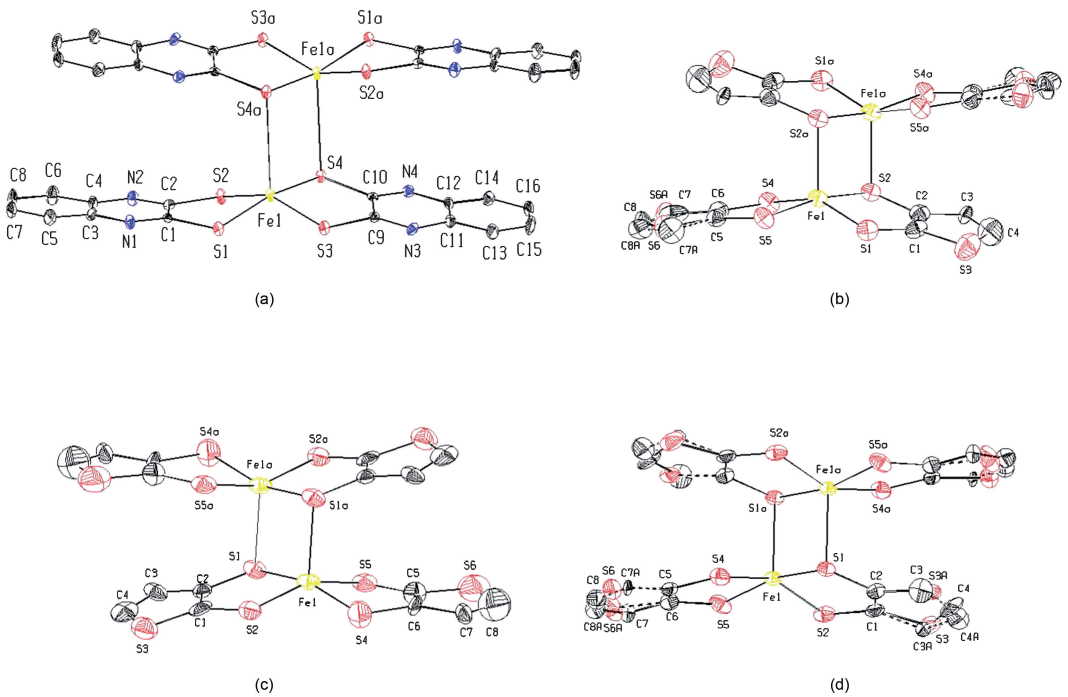

Fig. 1 ORTEP diagrams at the 40% probability level and atomic numbering schemes of : (a) $[Fe(qdt)_2]_2^{2-}$ in the crystal structure of $(BrBzPy)_2[Fe(qdt)_2]_2$ and $[Fe(\alpha\text{-}tpdt)_2]_2^{2-}$ in the crystal structure of (b) $(BrBzPy)_2[Fe(\alpha\text{-}tpdt)_2]_2$, (c) $(n\text{-}Bu_4N)_2[Fe(\alpha\text{-}tpdt)_2]_2$ and (d) $(Et_4N)_2[Fe(\alpha\text{-}tpdt)_2]_2$. Symmetry operations used in the dimer generation are $(1-x, -y, 1-z)$, $(-x, 1-y, 1-z)$, $(1-x, 1-y, -z)$ and $(1-x, -y, 1-z)$, respectively. Hydrogen atoms were omitted for clarity.

qdt ligand moieties are not only almost planar, with atomic rms deviations from their average planes smaller than 0.029 and 0.054 Å, but they are also almost coplanar with a small dihedral angle between them of 7.25(3)° (Fig. 2a). As discussed bellow, this coplanarity favours the arrangement of the dianions through stacking interactions into segregated columns.

The BrBzPy cation in $(BrBzPy)_2[Fe(qdt)_2]_2$ adopts a standard geometry, with the pyridine and the benzene rings, making a dihedral angle of 75.29(2)° and these rings make dihedral angles with the reference plane N5–C22–C23, of 73.97(4)° and 79.80(3)°, respectively (Fig. 3a). The BrBzPy cations are related by an inversion centre forming pairs in a clear P4AE (parallel fourfold aryl embrace),[11] where the pyridine rings are parallel at a ring centroid distance of 3.808(5) Å, allowing significant π–π interactions. Within the cation pair, a hydrogen atom from the pyridine fragment of one molecule interacts with the benzene ring fragment of the other molecule through a hydrogen bond (H distance to the benzene centroid is 2.56 Å). The cation packing mode in this crystal structure is different from all the other salts of this cation reported so far. While in other crystal structures the staking interactions within the cation were found to be, without exception, between the benzene fragment,[3a,3b,4a,12] in this complex the interacting moieties are pyridine rings, with the Br atoms of the benzene rings pointing outside the pair centre.

The supramolecular arrangement of $(BrBzPy)_2[Fe(qdt)_2]_2$ is similar to the one reported for $NO_2BzPy\,[Fe(mnt)_2]$[13] and consists of segregated columns of anion dimers and cation pairs along the *a* axis (Fig. 4a). In the $(BrBzPy)_2[Fe(qdt)_2]_2$ crystal structure the

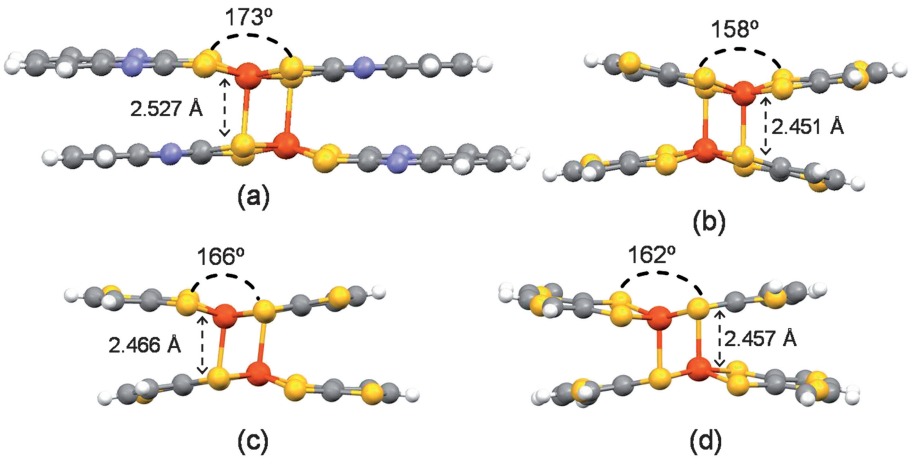

Fig. 2 Details showing (a) the $[Fe(qdt)_2]_2^{2-}$ in the crystal structure of $(BrBzPy)_2[Fe(qdt)_2]_2$, and the $[Fe(\alpha\text{-tpdt})_2]_2^{2-}$ in the crystal structure of (b) $(BrBzPy)_2[Fe(\alpha\text{-tpdt})_2]_2$, (c) $(n\text{-}Bu_4N)_2[Fe(\alpha\text{-tpdt})_2]_2$ and (d) $(Et_4N)_2[Fe(\alpha\text{-tpdt})_2]_2$. The values of the mean plane angle between the ligand moieties and the Fe–S apical bond lengths are indicated.

Table 1 Fe–S bond parameters in related Fe^{III} bisdithiolenes[a]

Compound	δFe/Å	Fe–S_{ap}/Å	<Fe–S>$_{bas}$/Å
$(BrBzPy)_2$ $[Fe(qdt)_2]_2$	0.310	2.527(12)	2.2255(12)
$(BrBzPy)_2[Fe(\alpha\text{-tpdt})_2]_2$	0.386	2.451(2)	2.242(2)
$(Et_4N)_2[Fe(\alpha\text{-tpdt})_2]_2$	0.384	2.4570(17)	2.2375(18)
$(n\text{-}Bu_4N)_2[Fe(\alpha\text{-tpdt})_2]_2$	0.373	2.466(4)	2.235(5)
$(n\text{-}Bu_4N)_2[Fe(dcbd)_2]_2$ [9]	0.370	2.4760(5)	2.2250(5)
$((ph)_4As)_2[Fe(qdt)_2]_2$ [2]	0.344	2.4884(12)	2.2338(13)
$(NO_2CH_3BzPy)_2[Fe(mnt)_2]_2$ [15]	0.385	2.4385(18)	2.2159(18)

[a] δFe = distance of Fe atom from the average basal S plane, Fe–S_{ap} = apical bond length, <Fe–S>$_{bas}$ = average basal bond lengths.

$Fe(qdt)_2$ complexes are more tightly stacked than in the $NO_2BzPy[Fe(mnt)_2]$ salt due the smaller distortion and larger coplanarity of the ligands. Indeed, along the column the iron dimers are connected by several short C···C contacts and one short Fe···S contact, with the two molecules slightly slipped along their major and minor axis, in a fashion similar to the one observed in the anions molecules within the dimer. Thus, apart from the alternated Fe–S apical bonds, the anion stacks are almost uniform (Fig. 4b,c). The cation pairs stack along *a* in a OFF (offset face-to-face) configuration, in such a way that the pyridine rings sit on top of each other at alternating distances of 3.415(4) Å and 3.437(4) Å (or ring centroid distances of 3.808(3) Å and 3.546(4) Å, giving rise to a chain of π–π interactions along *a* (Fig. 4d).

The iron dimers and the pairs of cations are connected by several strongly charged assisted hydrogen bonds; along *b*, while the benzene ring of the cations interacts with the anions through N···H–C hydrogen bonds, the pyridine ring connects to the anion *via* its sulfur atoms giving rise to several C–H···S hydrogen bonds (see table S1 in the ESI†). From the crystal packing we can see that the thickness along the staking direction of the dimer (~6.8 Å) and of the cation pair is almost the same, allowing a perfect fit of the two neighbouring columns, side-by-side (Fig. 4b–d)).

The related compound $(BrBzPy)_2[Fe(\alpha\text{-tpdt})_2]_2$ crystallises in the monoclinic space group *P*21/*c*. Its crystal structure is again composed of dimers of the $Fe(\alpha\text{-tpdt})_2$ anions and pairs of $(BrBzPy)^+$ cations. As usual, the $[Fe(\alpha\text{-tpdt})_2]_2^{2-}$ dianions exhibit

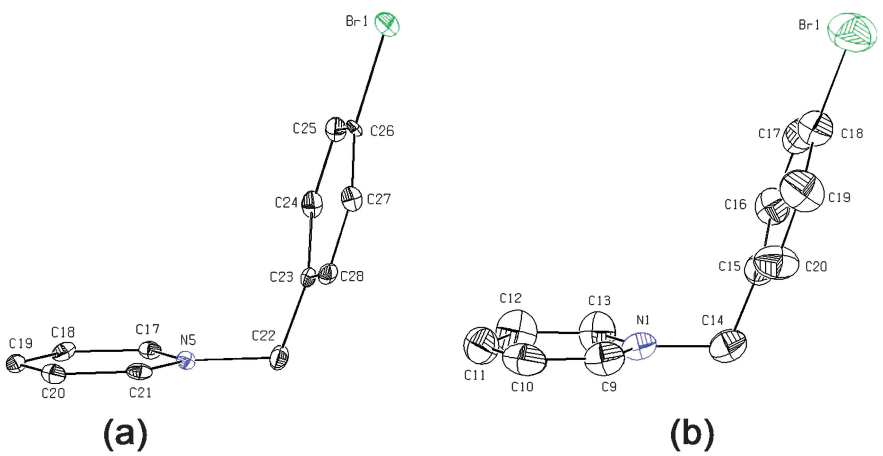

Fig. 3 ORTEP diagrams at the 40% probability level and atomic numbering schemes of the BrBzPy cations in the crystal structure of: (a) $(BrBzPy)_2[Fe(qdt)_2]_2$ and (b) $(BrBzPy)_2[Fe(\alpha\text{-tpdt})_2]_2$. Hydrogen atoms were omitted for clarity.

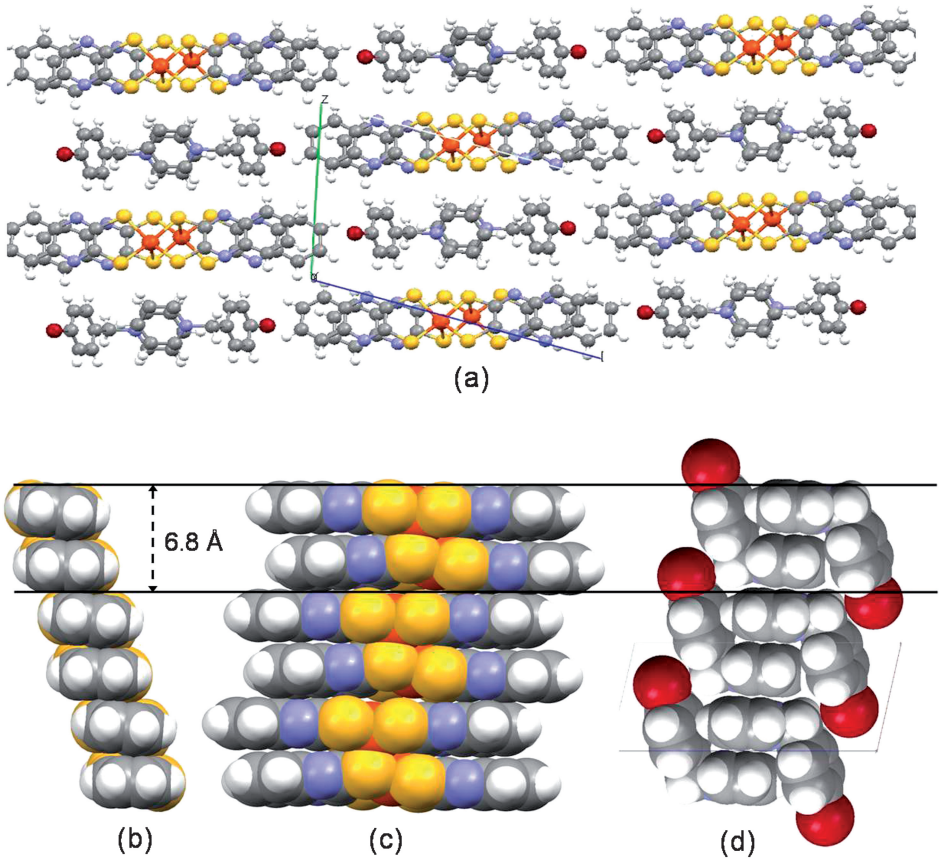

Fig. 4 (a) Crystal structure of $(BrBzPy)_2[Fe(qdt)_2]_2$, viewed along *a*; partial views showing an anionic stack (b) front view, along *c* and (c) side view, along [110]; (d) a cationic stack, viewed along *b*.

a dimeric arrangement with an inversion centre located between the two Fe atoms (Fig. 1b). However, in this case its geometry is essentially identical to all previously reported dimers of Fe^{III} bis-dithiolene complexes, the Fe atom being displaced towards the axial ligand 0.39 Å away from the S1, S2, S4 and S5 mean plane and with an Fe–S apical distance of 2.451(2) Å. Also as usual, the two ligands are not coplanar making a dihedral angle of 22.19(3)° (Fig. 2b). The two α-tpdt ligands present disorder in the position of the thiophenic sulfur atom. In one ligand this disorder could be modelled as resulting from a 55 : 45 occupation ratio of two positions involving atoms C7, C8 and S6. This ligand disorder is identical to that previously reported in different salts of square planar complexes of these (α-tpdt) ligands with other metals (*e.g.* Ni, Au, Pt, Co), resulting from a tendency to preferably adopt a *trans* configuration with orientation disorder. The only short contact within the dimer is observed between a coordination sulfur atom and one carbon atom from the thiophenic ring(S5···C2).

In $(BrBzPy)_2[Fe(\alpha\text{-tpdt})_2]_2$ the BrBzPy cation adopts a geometry close to that in BrBzPy $[Fe(qdt)_2]$, with the pyridine and the benzene rings creating a dihedral angle of 71.75(1)° and these rings creating dihedral angles with the reference plane N1–C14–C15, of 78.72(3)° and 88.22(3)°, respectively (Fig. 3b). Also, the packing mode of pairs is similar to the one observed in $(BrBzPy)_2[Fe(qdt)_2]_2$, a clear P4AE with the pyridine rings parallel at a ring centroid distance of 3.757(2) Å, indicative of clear π–π interactions and a hydrogen bond of 2.70 Å (H distance to the benzene centroid).

The crystal packing consists of parallel columns of alternating pair of cations and anion dimers, aligned along the [101] direction (Fig. 5). Along the columns several hydrogen bonds and short contacts between the cationic and anionic species are observed (see Table S2 in the ESI†), mainly involving the pyridine ring, which sits on top of one of the MS2C2 rings of the complex (the distance between the centroid rings is 3.747(4) Å). The bromine in the benzene ring also interacts with the anionic dimer through a charge assisted hydrogen bond.

It's worthwhile referring that the cation pair and the anionic dimer have comparable dimensions, well adjusted to the alternated stacking of cation pairs and dianion dimers (Fig. 5d). Neighbouring columns are linked through several short interactions and a few hydrogen bonds, mostly involving cations and anions. The only exception is the Br···H–C hydrogen bond between the neighbouring pair of cations, involving a bromine atom of one pair and a benzene ring of the other (the Br distance to the benzene ring centroid is 3.492(3) Å).

In these two structures with $[Fe(\alpha\text{-tpdt})_2]_2$ and $[Fe(qdt)_2]_2$ dianions it is observed that the $(BrBzPy)^+$ cation effectively induces the formation of stacks, but of different types depending on the ligand nature. In the first example, most probably due to the exceptional geometry of the $[Fe(qdt)_2]_2$ dimer with almost coplanar ligands and long apical bonds that naturally stack on top of each other, the most favourable packing is the observed anions and cation segregation in different columns, which have a good thickness match along the stacking axis, aligning perfectly

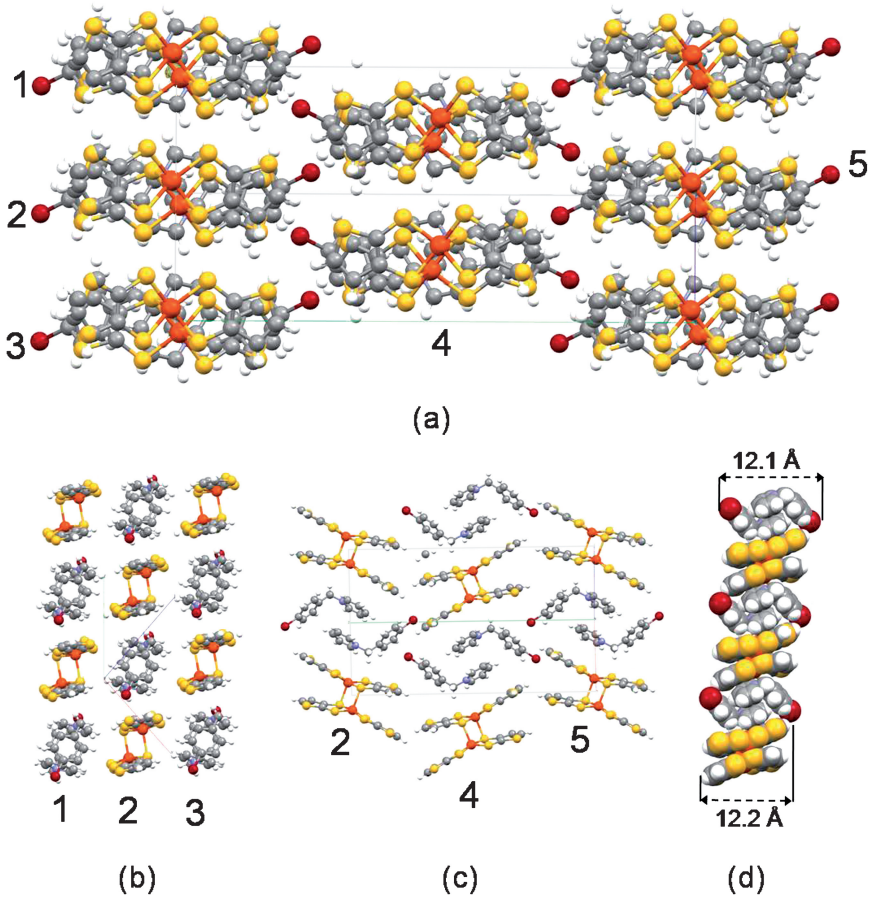

Fig. 5 (a) View of the crystal structure of $(BrBzPy)_2[Fe(\alpha\text{-tpdt})_2]_2$ along the [101] direction; partial views of selected columns (b) 1-2-3 along *c* and (c) columns 2-4-5 along *b*; (d) one mix column of alternated dianion dimers and pairs of cations.

side-by-side. In the second example mixed columns of alternating dimers and a pair of cations are observed. In this case, where the α-tpdt ligand is much smaller, we observe a good match on the dianion's and a pair of cation's dimensions, leading to a perfect adjustment of the molecules on top of each other. On the other hand, this dimer has the usual distorted geometry, hampering the regular stacking of the dianions.

This different tendency of the Fe complexes with these two ligands to dimerisation is also reflected in their different redox behaviour in solution. The cyclic voltammetry of $(BrBzPy)_2[Fe(\alpha\text{-tpdt})_2]_2$, in dichloromethane, as well as the other $Fe(\alpha\text{-tpdt})_2$ salts $(n\text{-}Bu_4N)_2[Fe(\alpha\text{-tpdt})_2]_2$ and $(Et_4N)_2Fe(\alpha\text{-tpdt})_2]_2$, show two pairs of symmetric redox waves, indicative of the reversible process centred at −0.065 V and +0.232 V *vs.* Ag/AgCl (Fig. 6). These closely spaced reversible waves are indicative of redox processes involving stable undissociated dimers in solution and can be ascribed to the couples $[Fe(\alpha\ tpdt)_2]_2^{3-}/[Fe(\alpha\ tpdt)_2]_2^{2-}$ and $[Fe(\alpha\text{-tpdt})_2]^{2-}/[Fe(\alpha\text{-tpdt})_2]_2^{-}$.

The redox behaviour of the $[Fe(qdt)_2]_2$ salt, in the same solvent, is quite distinct, showing a complex behaviour closer to some bisdithiolene complexes known to be partially dissociated in solution.[14] The only quasi-reversible process is seen at −0.474 V followed by further reduction waves which can be ascribed to the processes $[Fe(qdt)_2]^{2-}/[Fe(qdt)_2]^{-}$, 2 $[Fe(qdt)_2]^{2-}/[Fe(qdt)_2]_2^{-}$ or redox processes involving an equilibrium between different dimeric and dissociated species. Above 0.45 V other irreversible oxidation waves involving most probably the oxidation of dissociated $[Fe(qdt)_2]^{-}$species are visible.

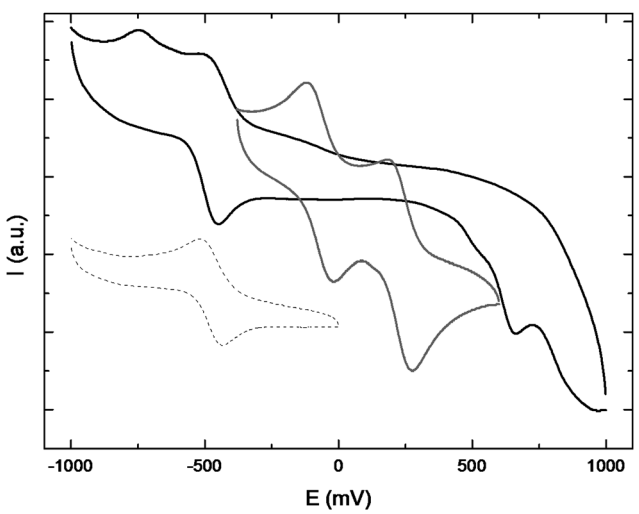

Fig. 6 Cyclic voltamograms of $(BrBzPy)_2[Fe(qdt)_2]_2$ (black line) and $(BrBzPy)_2[Fe(\alpha\text{-tpdt})_2]_2$ (gray line), versus Ag/AgCl, in dichloromethane. The dashed line shows in detail the quasi-reversible process at −0.474 V.

(n-$Bu_4N)_2[Fe(\alpha$-tpdt$)_2]_2$ and $(Et_4N)_2[Fe(\alpha$-tpdt$)_2]_2$

In order to understand the role of the cation in these crystal structures we also analyse the crystal packing of two [Fe(α-tpdt)$_2$] similar tetraalkyl salts: (n-$Bu_4N)_2[Fe(\alpha$-tpdt$)_2]_2$ and $(Et_4N)_2[Fe(\alpha$-tpdt$)_2]_2$.

The (n-$Bu_4N)_2[Fe(\alpha$-tpdt$)_2]_2$ salt crystallises in the monoclinic space group $P21/c$. Its crystal structure is again composed of dimers of $[Fe(\alpha\text{-tpdt})_2]^-$ anions (Fig. 1c). The $[Fe(\alpha\text{-tpdt})_2]_2^{2-}$ dianions exhibit a dimeric arrangement with an inversion centre located between the two Fe atoms, with a geometry virtually identical to the one observed in $(BrBzPy)_2Fe(\alpha\text{-tpdt})_2]_2$ salt. The Fe atom is displaced towards the axial ligand 0.373 Å away from the S1, S2, S4 and S5 mean plane and the Fe–S apical distance is 2.4664(2) Å. Also as usual, the two ligands are not coplanar making a dihedral angle of 14.10(5)° (Fig. 2c). Although it could not be well modelled, the two α-tpdt ligands present disorder in the position of the thiophenic sulfur atom. This crystal structure is organized in "pseudo" chains aligned along a. Along these isolated chains there are no short interactions. The space between the "chains" is filled by the $(n\text{-}Bu_4N)^+$ cations and its long aliphatic chains, which interact with the dianions on both sides, above and below, through several charge assisted $S_{coord}\cdots$H–C hydrogen bonds (Fig. 7, see Table S3 in the ESI†).

The $(Et_4N)_2[Fe(\alpha\text{-tpdt})_2]_2$ salt crystallises in the monoclinic space group $P21/n$. Its crystal structure is again composed of dimers of $Fe(\alpha\text{-tpdt})_2$ anions, identical to all previously described in this paper (Fig. 1d), with the Fe atom being displaced towards the axial ligand 0.384 Å away from the S1, S2, S4 and S5 mean planes and with an Fe–S apical distance of 2.4570(11) Å. Also, as found in the related compounds the two ligands are not coplanar creating a dihedral angle of 17.48(3) Å (Fig. 2d). The two α-tpdt ligands present disorder in the position of the thiophenic sulfur atom. This disorder could be modelised as resulting from 70 : 30 and 61 : 39 occupation ratios of two positions involving the atoms S3, C3 and C4 and S6, C7 and C8, respectively. The observed disorder is identical to all previously reported for this ligand.[4] Nevertheless, due to the smaller size of the cation, the crystal structure is quite distinct to the one observed for the (n-$Bu_4N)_2[Fe(\alpha$-tpdt$)_2]_2$ salt (and $(BrBzPy)_2[Fe(\alpha\text{-tpdt})_2]_2$ salt), with the dianionic dimers much closer to each other, originating a crystal packing with clear segregations of dianions and cations on layers (Fig. 8a). The anionic layer is tightly linked by a 2D network of charge assisted S···H–C hydrogen bonds between dimer extremities (Fig. 8b). The anionic and cationic layers are also connected by S···H–C hydrogen bonds involving all sulfur atoms of the dianion (see Table S4 in the ESI†).

These two crystal structures reveal that very small differences on the cation nature (they just differ on a CH_2–CH_2 fragment on each "arm") can reflect very different crystal packings. The smaller $(Et_4N)^+$ cation allows the anions to become closer and interact though several hydrogen bonds, giving rise to a 2D layer of contacts, while the relative $(n\text{-}Bu_4N)^+$, with its long arms pull the molecules apart and isolate the anionic species.

Experimental

General materials and methods

All procedures were carried out under strict anaerobic conditions under dry nitrogen or argon atmosphere unless otherwise stated. All solvents were purified following standard procedures. 2,3-Quinoxalinedithiol[15] and 5,6-thieno[2,3-d]-1,3-dithiol-2-one[4a] were synthesised as previously described. Other chemicals were commercially obtained and used without any further purification. IR spectra were obtained on a Perkin Elmer 577 spectrophotometer. Cyclic voltammetry data were obtained using a BAS C3 Cell Stand. The measurements were performed at room temperature in dichloromethane solutions containing nBu$_4$NPF$_6$ as supporting electrolyte, with a scan rate of 100 mV s^{-1}, platinum wire working- and counter-electrodes and using Ag/AgCl as a reference electrode.

Synthesis of complexes

$(BrBzPy)_2[Fe(qdt)_2]_2$. 2,3-Quinoxalinedithiol (0.62 g, 0.0032 mol) was added to a solution of metallic sodium (0.16 g, 0.0069) in methanol (10 mL). The resulting solution was stirred at room temperature, then a solution of of $FeCl_3$ (0.26 g, 0.0016 mol) in methanol (5 mL) was added dropwise over a period of 15 min.

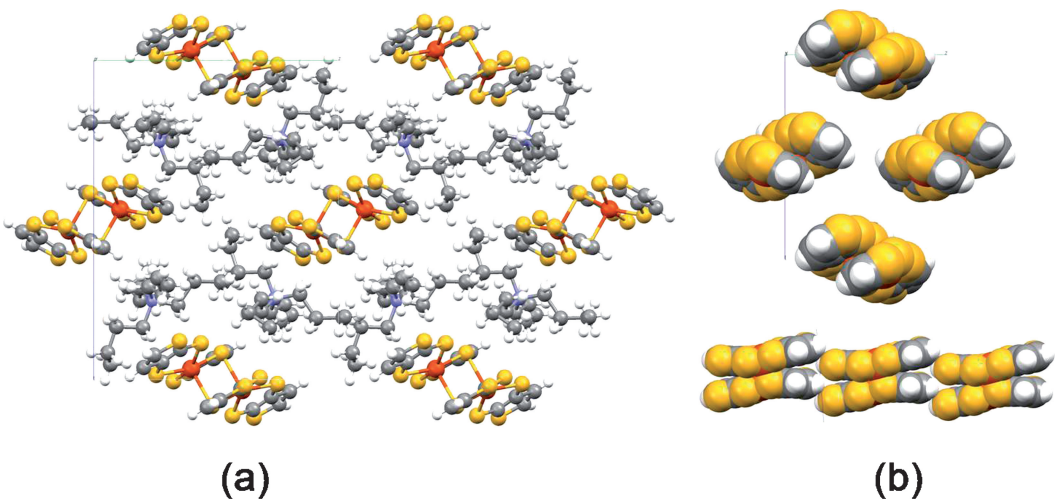

Fig. 7 (a) View of the crystal structure of (n-$Bu_4N)_2Fe(\alpha$-tpdt$)_2]_2$ along a; (b) partial view along a, showing an anionic network (up) and one anionic "chain" (down).

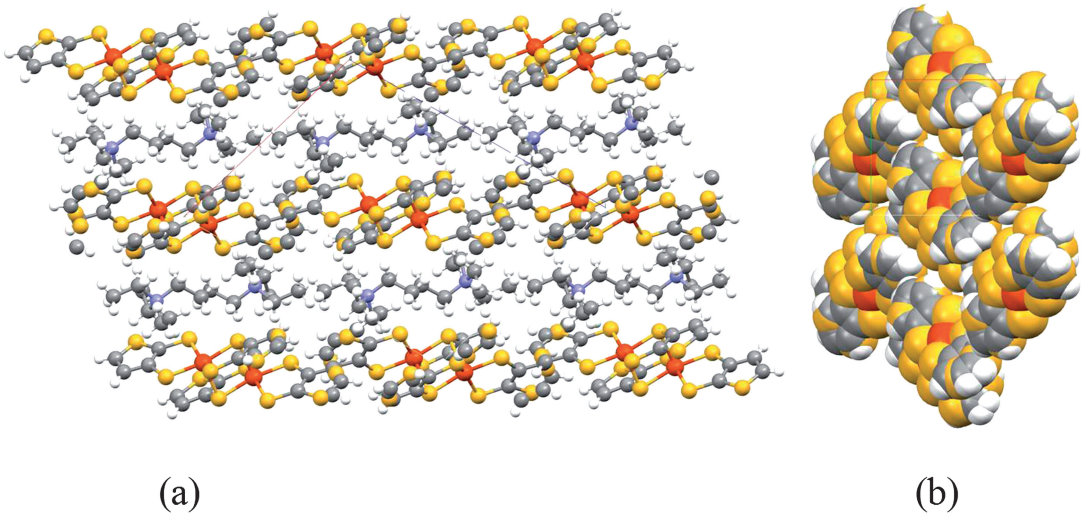

Fig. 8 (a) View of the crystal structure of $(Et_4N)_2[Fe(\alpha\text{-tpdt})_2]_2$ along *b*; (b) partial view of one anionic layer along *c*.

The final solution was filtered directly to a methanol (5 mL) solution of 1-(4′-bromobenzyl)pyridinium bromide (0.52 g, 0.0016 mol). An equal volume of water was added and the mixture was kept at 5 °C for one week. A dark crystalline precipitate was obtained by filtration. The product was purified by dissolution in methanol with a few drops of ammonia and precipitation by addition of an equal volume of water. Shiny black crystals were collected by filtration after one week at 5 °C. Single crystal was obtained by slow evaporation of a methanolic solution under nitrogen. Yield 38% (0,380 g) mp 190 °C. CHNS ($C56H38N10S8Fe_2Br_2$): calc. C 48.90, H 2.62, N 10.19, S 18.63; found C, 48.59, H, 2.72, N 9.91, S 18.43; υ = 3100 (w, Ar–H), 1480, 1470 (w, C=N), 615 (w, C–Br), 420 (m, S–Fe) cm-1.

$(BrBzPy)_2[Fe(\alpha\text{-tpdt})_2]_2$. To a solution of potassium metoxide in methanol (10 ml, 0.2 M) was added, under stirring, 5,6-thieno[2,3-d]-1,3-dithiol-2-one (100 mg, 5.7×10^{-4} mol). The formed yellow solution was filtered and added to a solution of iron(III) chloride (95 mg, 2.9×10^{-4} mol) in methanol (5 mL), turning to a dark mixture. The inorganic precipitate was removed and the liquor added to a solution of 1-(4′-bromobenzyl)pyridinium bromide (385 mg, 2.9×10^{-4} mol) in methanol (5 mL). Immediately a fine, shiny dark solid precipitated. The solid obtained was filtered and recrystallised from acetonitrile, to afford dark plates. Yield 71% (123 mg).CHNS ($C_{40}H_{30}N_2S_{12}Fe_2Br_2$): calcd. C 40.21, H 2.53, N 2.34, S 32.20; found C 39.07, H 2.30, N 2.23, S 31.75.

$(n\text{-}Bu_4N)_2[Fe(\alpha\text{-tpdt})_2]_2$. The compound was prepared using the same method as for $(BrBzPy)_2[Fe(\alpha\text{-tpdt})_2]_2$, using n-Bu_4NBr instead of BrBzPyBr. Crystals suitable for X-ray measurements were obtained after recrystalization from 1 : 1 CH_2Cl/*n*-henanes solutions. Yield 80% (67.5 mg).CHNS ($C_{48}H_{80}N_2S_{12}Fe_2$): calcd. C 48.79, H 6.82, N 2.37, S 32.56; found C 48.42, H 6.72, N 2.50, S 32.46.

$(Et_4N)_2[Fe(\alpha\text{-tpdt})_2]_2$. The compound was prepared using the same method as for $(BrBzPy)_2[Fe(\alpha\text{-tpdt})_2]_2$, using Et_4Br instead of BrBzPyBr. The product was obtained as dark plate crystals, directly from the synthesis, after allowing the final solution to rest overnight. Yield 75% (52.8 mg). CHNS ($C_{32}H_{48}N_2S_{12}Fe_2$): calcd. C 40.16, H 5.05, N 2.93, S 40.19; found C 40.84, H 5.20, N 3.07, S 40.63.

X-Ray crystallography

X-Ray diffraction experiments were performed with a Bruker AXS APEX CCD detector diffractometer using graphite monochromated Mo Kα radiation (λ = 0.71073 Å), in the φ and ω scans mode. A semiempirical absorption correction was carried out using SADABS.[16] Data collection, cell refinement and data reduction were done with the SMART and SAINT programs.[17] The structures were solved by direct methods using SIR97[18] and refined by full-matrix least-squares methods using the program SHELXL97,[19] using the winGX software package.[20] Non-hydrogen atoms were refined with anisotropic thermal parameters whereas H-atoms were placed in idealized positions and allowed to refine riding on the parent C atom.‡ Molecular graphics were prepared using ORTEP 3.[21]

‡ **Crystallographic data for $(BrBzPy)_2[Fe(qdt)_2]_2$**: $C_{56}H_{38}N_{10}S_8Fe_2Br_2$, M = 1378.98 g mol^{-1}, triclic, space group P-1, a = 7.3129(4) Å, b = 11.4865(7) Å, c = 17.0461(11) Å, α = 100.625(3)°, β = 98.672(3)°, γ = 106.991(3)°, U = 1313.60(14) Å^3, Z = 1, D_c = 1.743 g cm^{-3}, μ(Mo Kα) = 2.444 mm^{-1}, 11335 reflections measured, 4957 unique, final $R(F^2)$ = 0.0424 using 3157 reflections with $I > 2.0\sigma(I)$, R(all data) = 0.0933, T = 150(2) K. CCDC 695833. **Crystallographic data for $(BrBzPy)_2[Fe(\alpha\text{-tpdt})_2]_2$**: $C_{40}H_{30}N_2S_{12}Fe_2Br_2$, M = 1194.92 gmol^{-1}, monoclinic, space group $P2_1/c$, a = 9.3573(5) Å, b = 25.3284(12) Å, c = 10.0811(6) Å, β = 100.854(3)°, U = 2346 (2) Å^3, Z = 2, D_c = 1.691 g cm^{-3}, μ(Mo Kα)= 2.888 mm^{-1}, 19152 reflections measured, 4116 unique, final $R(F^2)$ = 0.0583 using 1964 reflections with $I > 2.0\sigma(I)$, R(all data) = 0.1621, T = 150(2) K. CCDC 695835. **Crystallographic data for $(n\text{-}Bu_4N)_2[Fe(\alpha\text{-tpdt})_2]_2$**: $C_{48}H_{80}N_2S_{12}Fe_2$, M = 1181.58 g mol^{-1}, monoclinic, space group $P2_1/c$, a = 12.593(3) Å, b = 13.734(3) Å, c = 17.690(3) Å, β = 97.430(11)°, U = 3033.8(10) Å^3, Z = 2, D_c = 1.293 g cm^{-3}, μ(Mo Kα) = 0.923 mm^{-1}, 18378 reflections measured, 4339 unique, final $R(F^2)$ = 0.1322 using 1637 reflections with $I > 2.0\sigma(I)$, R(all data) = 0.3038, T = 150(2) K. CCDC 695832. **Crystallographic data for $(Et_4N)_2[Fe(\alpha\text{-tpdt})_2]_2$**: $C_{32}H_{28}N_2S_{12}Fe_2$, M = 957.16 g mol^{-1}, monoclinic, space group $P2_1/n$, a = 12.5925(6) Å, b = 11.0890(5) Å, c = 16.2457(8) Å, β = 106.464(3)°, U = 2175.51(18) Å^3, Z = 2, D_c = 1.461 g cm^{-3}, μ(Mo Kα) = 1.269 mm^{-1}, 15151 reflections measured, 4131 unique, final $R(F^2)$ = 0.0627 using 2219 reflections with $I > 2.0\sigma(I)$, R(all data) = 0.1424, T = 150(2) K. CCDC 695834.

Conclusions

In conclusion, the iron complexes with qdt and α-tpdt ligands respond to the presence of the bromobenzylpyridinium cation, by making in the solid state structures based on column stackings. For the qdt ligand segregated anionic and cationic columns are formed in a way similar to other transition metal bisdithiolene salts with related bezylpyridinium cations. For the α-tpdt ligand there are columns made of mixed pairs of cations and anion dimers.

However, while the α-tpdt ligand leads to stable dimerised dianionic species $[Fe(\alpha\text{-tpdt})_2]_2^{2-}$ with geometric parameter values within the range of typical Fe(III) dimeric species, the qdt ligand demonstrates its unique character of being able to form a $[Fe(qdt)_2]_2^{2-}$ structure with weaker dimerisation. This dimerisation is in-between the monomeric species found so far only in the related salt with this ligand, n-Bu_4N $[Fe(qdt)_2]$, and the usual Fe(III) bisdithiolene dimers also displayed by an Fe complex with this ligand in its tetraphenylphosphonium salt.

The different stability of the Fe-bisdithiolene dimeric complexes with these two ligands is also confirmed by electrochemical studies, showing quite stable $[Fe(\alpha\text{-tpdt})_2]_2^{n-}$ dimers in solution ($n = 1, 2, 3$), while the qdt analogues easily dissociate.

Acknowledgements

This work was partially supported by Fundação para a Ciência e Tecnologia (Portugal) under contracts POCI/QUI/57528/2004 and PDCT/QUI/64967/2006.

References

1 (*a*) J. A. McCleverty, *Prog. Inorg. Chem.*, 1968, **10**, 49; (*b*) D. Coucuvanis, *Prog. Inorg. Chem.*, 1970, **11**, 233; (*c*) R. Eisenberg, *Prog. Inorg. Chem.*, 1971, **12**, 295; (*d*) S. Alvarez, V. Ramon and R. Hoffman, *J. Am. Chem. Soc.*, 1985, **107**, 6253; (*e*) K. D. Karlin and E. I. Stiefell, *Prog. Inorg. Chem.*, 2004.
2 D. Simão, J. A. Ayllón, S. Rabaça, M. J. Figueira, I. C. Santos, R. T. Henriques and M. Almeida, *CrystEngComm*, 2006, **8**, 658.
3 (*a*) J. L. Xie, X. M. Ren, C. He, Y. Song, C. Y. Duan, S. Gao and Q. J. Ming, *Polyhedron*, 2003, **22**, 299–305; (*b*) X. M. Ren, H. Okudera, R. K. Kremer, Y. Song, C. He, Q. J. Meng and P. H. Wu, *Inorg. Chem*, 2004, **43**, 2569–2576; (*c*) Z. Ni, X. M. Ren, J. Ma, J. Xie, C. Ni, Z. Chen and Q. Meng, *J. Am. Chem. Soc.*, 2005, **127**, 14330.
4 (*a*) D. Belo, H. Aves, E. B. Lopes, M. T. Duarte, V. Gama, R. T. Henriques, M. Almeida, E. Ribera, C. Rovira and J. Veciana, *Chem.–Eur. J.*, 2001, **7**, 511; (*b*) D. Belo, H. Alves, S. Rabaça, L. C. Pereira, M. T. Duarte, V. Gama, R. T. Henriques, M. Almeida, E. Ribera, C. Rovira and J. Veciana, *Eur. J. Inorg. Chem.*, 2001, **12**, 3127; (*c*) D. Belo, M. J. Figueira, J. Mendonça, I. C. Santos, M. Almeida, R. T. Henriques, M. T. Duarte, C. Rovira and J. Veciana, *Eur. J. Inorg. Chem*, 2005, **16**, 3337; (*d*) D. Belo, M. J. Figueira, J. P. M. Nunes, I. C. Santos, L. C. Pereira, V. Gama, M. Almeida and C. Rovira, *J. Mater. Chem.*, 2006, **16**, 2746; (*e*) D. Belo, J. Mendonça, I. C. Santos, L. C. J. Pereira, M. Almeida, J. J. Novoa, C. Rovira, J. Veciana and V. Gama, *Eur. J. Inorg. Chem.*, 2008, **34**, 5327.
5 (*a*) W. C. Hamilton and I. Bernal, *Inorg. Chem.*, 1967, **11**, 2003; (*b*) J. V. Rodriguess, I. C. Santos, V. Gama, R. T. Henriques, J. C. Waerenborgh, M. T. Duarte and M. Almeida, *J. Chem. Soc., Dalton Trans.*, 1994, **18**, 2655.
6 B. S. Kang, L. H. Weng and D. X. Wu, *Inorg. Chim. Acta*, 1988, **148**, 147.
7 K. Awaga, L. H. Okuno, Y. Maruyama, A. Kobayashy, H. Kobayashy, S. Schenk and A. E. Underhill, *Inorg. Chem.*, 1994, **33**, 5598.
8 S. Tanaka and G. Matsubayashy, *J. Chem. Soc., Dalton Trans.*, 1992, **19**, 2837.
9 H. Alves, D. Simão, H. Novais, I. C. Santos, C. Giménez-Saiz, V. Gama, J. C. Waerenborgh, R. T. Henriques and M. Almeida, *Polyhedron*, 2003, **22**, 2481–2486.
10 A. C. Cerdeira, D. Simão, I. C. Santos, A. Machado, L. C. J. Pereira, J. C. Waerenborgh, R. T. Henriques and M. Almeida, *Inorg. Chim. Acta*, 2008, **361**, 3836–3841.
11 X. M. Ren, P. H. Wu and W. W. Zhang, *Trans. Metal. Chem.*, 2002, **27**, 394.
12 (*a*) V. Russel, M. Scudder and I. Dance, *J. Chem. Soc., Dalton Trans.*, 2001, 789; (*b*) C. Janiak, *J. Chem. Soc., Dalton Trans.*, 2000, 3885.
13 (*a*) X. Ren, Q. Meng, Y. Song, C. Lu and C. Hu, *Inorg. Chem.*, 2002, **41**, 5686; (*b*) Y.-C. Chen and X.-M. Ren, *Acta Crystallogr., Sect. E: Struct. Rep.Online*, 2005, **61**, m2176; (*c*) C. Ni, D. Dang, Z. Ni, Y. Li, J. Xie, Q. Meng and Y. Yao, *J. Coord. Chem.*, 2004, **57**, 1529; (*d*) X. Ren, J. Ma, C. Lu, S. Yang, Q. Meng and P. Wu, *Dalton Trans.*, 2003, 1345; (*e*) W.-J. Tong, L. Liu, Q.-J. Meng and Y.-Z. Li, *Acta Crystallogr., Sect. E: Struct. Rep. Online*, 2002, **58**, m724; (*f*) H. Xu and X.-M. Ren, *Acta Crystallogr., Sect. E: Struct. Rep. Online*, 2006, **62**, m3134; (*g*) J. Xien, X. Ren, Z. Ni, W. Zhang, Y. Yac and Q. Meng, *J. Chem. Crystallogr.*, 2003, **33**, 65.
14 A. L. Balch, I. G. Dance and R. H. Holm, *J. Am. Chem. Soc.*, 1968, **28**, 1139.
15 L. J. Theriot, K. K. Ganguli, S. Kavarnos and I. Bernal, *J. Inorg. Nucl. Chem.*, 1969, **31**, 133.
16 G. M. Sheldrick, *SADABS*, Bruker AXS Inc., Madison, WI, USA, 2004.
17 Bruker. *SMART and SAINT*.Bruker AXS Inc., Madison, WI, USA, 2004.
18 A. Altomare, M. C. Burla, M. Camalli, G. Cascarano, G. Giacovazzo, A. Guagliardi, A. G. G. Moliterni, G. Polidori and R. Spagna, *J. Appl. Crystallogr.*, 1999, **32**, 115.
19 G. M. Sheldrick, *SHELXL97, Program for Crystal Structure Refinement*, University of Göttingen, Germany, 1997.
20 L. J. Farrugia, *J. Appl. Crystallogr.*, 1999, **32**, 837.
21 L. J. Farrugia, *J. Appl. Crystallogr.*, 1997, **30**, 565.